

## Inertial Range Scalings of Dissipation and Enstrophy in Isotropic Turbulence

Shiyi Chen,<sup>1,2</sup> Katepalli R. Sreenivasan,<sup>3</sup> and Mark Nelkin<sup>4</sup>

<sup>1</sup>IBM Research Division, T. J. Watson Research Center, P.O. Box 218, Yorktown Heights, New York 10598

<sup>2</sup>Theoretical Division and Center for Nonlinear Studies, Los Alamos National Laboratory, Los Alamos, New Mexico 87545

<sup>3</sup>Mason Laboratory, Yale University, New Haven, Connecticut 06520-8286

<sup>4</sup>Physics Department, New York University, New York, New York 10003  
and Levich Institute, CCNY, New York, New York 10031

(Received 24 April 1997)

The inertial range scalings of local averages of energy dissipation rate and enstrophy (vorticity squared) are studied using high resolution direct numerical simulation data for homogeneous and isotropic turbulence. The Taylor microscale Reynolds number is 216. It is found that the enstrophy is more intermittent than dissipation, consistent with previous one-dimensional surrogate measurements at high Reynolds numbers. Contrary to some recent expectations, enstrophy and dissipation have different exponents. [S0031-9007(97)03795-2]

PACS numbers: 47.27.Gs

An important step in the understanding of small-scale turbulence was the introduction [1] of the locally averaged dissipation rate,  $\varepsilon_r(\mathbf{x}, t) = V_r^{-1} \int_{V_r} \varepsilon(\mathbf{x}') d\mathbf{x}'$ , where  $\varepsilon$  is the rate of dissipation per unit volume of the turbulent kinetic energy, and the volume of integration,  $V_r$ , is centered at  $\mathbf{x}$  and has a characteristic length scale  $r \ll L$ ,  $L$  being a suitable measure of the large-scale of turbulence. One can similarly define the local averages of enstrophy ( $= \omega^2$  where the vorticity  $\omega = \nabla \times \mathbf{u}$ ). The global averages of enstrophy and dissipation are related (i.e.,  $\langle \varepsilon \rangle = \nu \langle \omega^2 \rangle$ , where  $\nu$  is the kinematic viscosity coefficient of the fluid), but this does not imply that their local averages scale identically. If they do, however, there is some hope that the scaling exponents for small-scale turbulence are unique. If not, there is a need to identify classes of small-scale quantities which have the same scaling properties. Existing experimental data, surveyed in [2], suggest that the scaling exponents for dissipation and enstrophy may indeed not be the same, but the conclusion was not definitive because the experimental evidence was affected in unknown ways by artifacts such as Taylor's hypothesis and the use of one-dimensional surrogates of dissipation and vorticity; for example, it is known [3] that there are some differences between the energy dissipation and its one-dimensional surrogate.

Given the uncertain nature of the existing knowledge, it seemed important to study the scaling of enstrophy and dissipation without resorting to the artifacts just mentioned. We use direct numerical simulation of the Navier-Stokes equations carried out in a  $512^3$  periodic box [4]. A statistically steady state was obtained by forcing low Fourier modes. At the modest Reynolds number of this flow (the Taylor microscale Reynolds number,  $R_\lambda$ , is 216), a narrow inertial range can be identified by demonstrating that Kolmogorov's  $-4/5$  law [5] is verified [6].

For later purposes, note that the dissipation rate  $\varepsilon$  is related to the symmetric part of the strain tensor as  $\varepsilon = 2\nu S^2$ , where  $S^2 = S_{ij}S_{ji}$  and  $S_{ij} = 1/2(\partial u_i/\partial x_j +$

$\partial u_j/\partial x_i)$ . The relationship between  $S$  and the enstrophy,  $\Omega = \omega^2$ , is

$$S^2 = \frac{\Omega}{2} + \frac{\partial u_i}{\partial x_j} \frac{\partial u_j}{\partial x_i}. \quad (1)$$

Using the Navier-Stokes equations, the right-hand side of (1) can also be related to the pressure  $p$  via  $S^2 = \frac{\Omega}{2} - \nabla^2 p$ . The local averages of (1),  $S_r^2$  and  $\Omega_r$ , are connected through surface integrations as  $S_r^2 = \frac{\Omega_r}{2} + V_r^{-1} \int_{s(r)} \frac{\partial u_i u_j}{\partial x_j} ds_i$ , where  $s(r)$  denotes the surface around the volume  $V_r$ . From the above equations, we note that in general the power law scaling in the inertial range of  $\langle \varepsilon_r^p \rangle$  is not necessarily the same as that of  $\langle \Omega_r^p \rangle$ . On the other hand, the above equation does not at present point to fruitful results and yield predictions for the scaling relations of  $\langle \varepsilon_r^p \rangle$  and  $\langle \Omega_r^p \rangle$ . It is therefore useful to summarize the available experimental data and the phenomenological understanding.

Siggia [7] and Kerr [8] used direct simulations data to study the flatness of  $|S|$  and  $|\omega|$  and found the latter to be larger, implying that the  $\Omega$  field is more intermittent than the  $\varepsilon$  field. The one-dimensional measurements of the streamwise components of  $\varepsilon$  and  $\omega$ , obtained at both high and low Reynolds numbers [9], conclude that the degrees of intermittency in the dissipation and enstrophy fields are not the same. Recent analysis of circulation data [10] implies that there are differences between the two scalings. Working from the spatial support of the dissipation and enstrophy, Wu and Fan [11] argue that the surface integration  $\int_{s(r)} \frac{\partial u_i u_j}{\partial x_j} ds_i$  is the major reason why  $\varepsilon_r$  is less intermittent. Finally, Chen *et al.* [12] have shown that the flatness of  $|\omega|$  is larger than that of  $|S|$  if the velocity field satisfies the quasinnormal assumption. On the other hand, a popular turbulence model [13] implicitly assumes that high-order statistics of the enstrophy and dissipation are the same in the inertial range; the hierarchy hypothesis in the model is based on moments of the locally

averaged dissipation while the codimension is taken from enstrophy. Most recently [14], it has been suggested from considerations of fusion rules that the inertial range scalings of local averages of all quantities within the same symmetry group should have the same scaling in the inertial range; a typical implication is that  $\langle \epsilon_r^p \rangle$  and  $\langle \Omega_r^p \rangle$  should possess the same scaling properties.

The available information is thus quite contradictory and the issue requires clarification. This is important because the answer bears on further theoretical development, and on the possibility or otherwise of a unique set of scaling exponents for small-scale turbulence. We shall therefore examine the relation between the statistical quantities  $\langle \epsilon_r^p \rangle$  and  $\langle \Omega_r^p \rangle$  for various values of  $p$  without using Taylor's hypothesis and one-dimensional surrogates; we shall also examine the scaling of fourth order tensor quantities related to those discussed in [14].

In Fig. 1, we show various normalized probability density functions (PDF's),  $\langle D_r \rangle P(D_r / \langle D_r \rangle)$ , as functions of the normalized quantity,  $D_r / \langle D_r \rangle$ , where  $D_r$  represents the local average of either the dissipation or the enstrophy; the averaging scale is within the inertial range. The PDF for the unaveraged dissipation and enstrophy are also shown. The PDF's for enstrophy possess wider tails than those of dissipation, indicating that large amplitude events in the enstrophy field are more prevalent than in the dissipation field. This is consistent with the observation that iso-surfaces of dissipation are more fragmented than iso-surfaces of enstrophy. In the inset we show the flatness of local averages of dissipation and enstrophy as functions of the averaging scale,  $r$ . It is seen that enstrophy's flatness is significantly larger than that of dissipation, especially in the dissipation range; in particular, for flatnesses, we have  $\langle \Omega^4 \rangle / \langle \Omega^2 \rangle^2 = 179$  and  $\langle \epsilon^4 \rangle / \langle \epsilon^2 \rangle^2 = 34.5$ , qualitatively consistent with previous

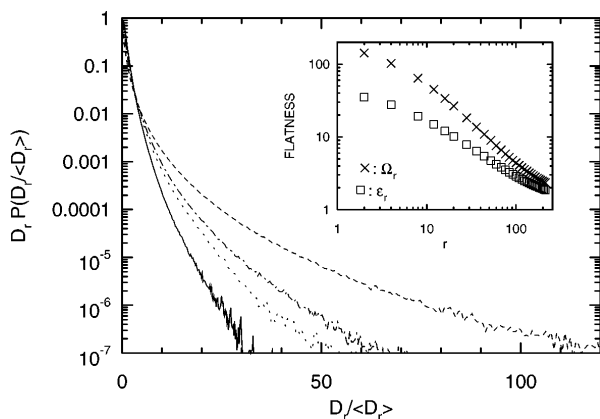


FIG. 1. Normalized PDF's  $D_r P(D_r / \langle D_r \rangle)$  as functions of  $D_r / \langle D_r \rangle$ . The solid line is for  $D_r = \epsilon_r$ , and the dotted line for  $D_r = \Omega_r$ . Here  $r = 16$  in units of lattice spacing, and lies in the inertial range. The dot-dashed line is for  $\epsilon$  while the dashed line is for  $\Omega$  (both with no space averaging). The inset shows the flatness of  $\epsilon_r$  and  $\Omega_r$  as functions of  $r$ .

findings [8]. Only when  $r$  approaches the box size of simulation do the two fields reach the common value of 1.

We have also compared the PDF's of dissipation and enstrophy with the lognormal distribution by examining the statistics of  $w_D = (\ln D - \langle \ln D \rangle) / \langle (\ln D - \langle \ln D \rangle)^2 \rangle^{1/2}$ . We found that  $(F_4)_\Omega = 3.33$ ,  $S_\Omega = -0.34$ ,  $(F_6)_\Omega = 21.86$ , and  $(F_4)_\epsilon = 3.07$ ,  $S_\epsilon = -0.1$ ,  $(F_6)_\epsilon = 16.54$ . Here  $F_4$ ,  $S$ , and  $F_6$  represent the flatness factor, the skewness, and the sixth order moment of  $w_D$ . These numbers also reflect the fact that the dissipation is close to a lognormal distribution and the enstrophy is more strongly intermittent than dissipation.

From three-dimensional visualization of turbulence structures at moderate Reynolds numbers [15], it is known that isosurfaces of high intensity events of dissipation wrap around those of high intensity events of enstrophy, the latter forming elongated tube-like structures [16,17]. It has been also argued from  $\Delta p = \Omega^2 / 2 - S^2$  that enstrophy concentration acts as a source of low pressure, which provides a method for visualizing vorticity structures experimentally [18]. The spatial correlation between dissipation and enstrophy can be quantified by means of conditional statistics. In Fig. 2,  $\langle \Omega_r' | \epsilon_r' \rangle$  (the  $\square$  symbol) and  $\langle \Omega_r'^2 | \epsilon_r' \rangle$  (the  $\times$  symbol) are shown as functions of  $\epsilon_r'$  for  $r$  in the inertial range, where quantities with prime are normalized by their mean values:  $\Omega_r' = \Omega_r / \langle \Omega \rangle$  and  $\epsilon_r' = \epsilon_r / \langle \epsilon \rangle$ . The dotted line refers to a linear variation and the dash-dotted line to a power of 2. It is evident that for all  $r$ , the moments of  $\Omega_r'$  increase with  $\epsilon_r'$ . Although the data do not correspond to any power law for small  $\epsilon_r'$ , the conditional averages for large  $\epsilon_r'$  grow linearly with  $\epsilon_r'$ . This result is consistent with visualization studies which show that the high amplitudes in  $\Omega_r'$  and  $\epsilon_r'$  possess a strong domain correlation. In the inset of Fig. 2, we plot the conditional statistics  $\langle \epsilon_r'^p | \Omega_r' \rangle$

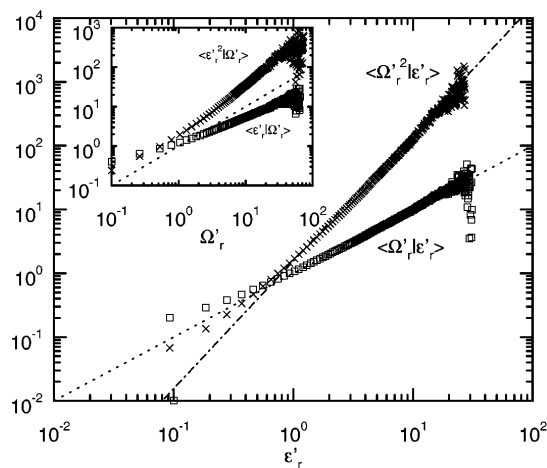


FIG. 2. Conditional statistics of  $\langle \Omega_r'^p | \epsilon_r' \rangle$  (for  $p = 1$  and 2) as functions of  $\epsilon_r'$  for  $r = 16$  lattice unit. The dotted line and the dash-dotted line represent power relation exponents of 1 and 2, respectively. The inset shows the conditional statistics of  $\langle \epsilon_r'^p | \Omega_r' \rangle$ . The dotted line represents a power of 1.

for a given  $\Omega_r^l$  for  $p = 1$  and  $2$ . For high amplitudes of  $\Omega_r^l$ ,  $\langle \varepsilon_r^l | \Omega_r^l \rangle$  grows slower than linearly (represented by the dotted line) and  $\langle \varepsilon_r^{l2} | \Omega_r^l \rangle$  grows slower than  $\Omega_r^{l2}$ . In fact, the measured exponents in the power range are close to  $0.6$  and  $1.2$  for  $p = 1$  and  $2$ , respectively.

We have also studied conditional averages for other  $p$  values and for different separations. In general, we find that  $\langle \Omega_r^p | \varepsilon_r^l \rangle \sim \varepsilon_r^{lp}$  for large  $\varepsilon_r^l$  values. The reversed conditional statistics,  $\langle \varepsilon_r^l | \Omega_r^p \rangle$ , seem to scale well with  $\Omega_r^{\alpha p}$  for the large  $\Omega_r^l$  region, with  $\alpha < 1$ . This implies that the spatial growth of  $\varepsilon_r^l$  in the statistical sense is slower than that of  $\Omega_r^l$ . The difference between the conditional statistics of  $\langle \Omega_r^p | \varepsilon_r^l \rangle$  and  $\langle \varepsilon_r^l | \Omega_r^p \rangle$  is consistent with visualization observations that dissipation and enstrophy are not correlated point by point though there is a strong domain correlation. It should be pointed out further that, for both sets of conditional statistics, the linear region shrinks with increasing of  $p$ .

In the inset to Fig. 3, we plot the moments  $\langle \varepsilon_r^{p/3} \rangle$  as functions of  $r$  for  $p = 1, 2, \dots, 10$  (from the top line to the bottom line). A power-law range for  $\langle \varepsilon_r^{p/3} \rangle \sim r^{\tau_{p/3}}$  can be identified between  $12$  and  $50$  lattice units, corresponding to  $0.147 \leq r \leq 0.613$  in units of  $2\pi$  for the whole box. Using data within the scaling range, the local slope  $\tau_{p/3}(r) = d\langle \varepsilon_r^{p/3} \rangle / d \ln r$  can be calculated as a function of  $r$  using a least-square fit for every three neighboring points. The averaged value of  $\tau_{p/3}$  is used as the scaling exponent in the inertial range; these numbers are shown in the plot by the (●) symbol. The error bar is too small to be noted. Some typical values of  $\tau_{p/3}$

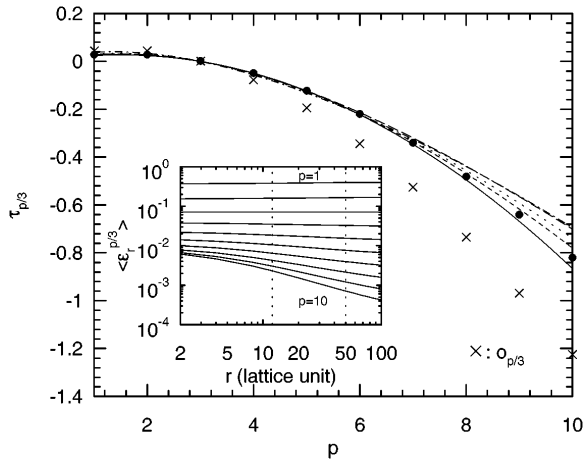


FIG. 3. The scaling exponents of  $\langle \varepsilon_r^{p/3} \rangle$  as a function of  $p$  from numerical measurement (●) and theoretical predictions from various phenomenological models: the solid line is for Kolmogorov's refined similarity theory [1], the dash-dotted line for the  $p$  model [19], the dotted line for She-Leveque model [13], the dashed line from Chen and Cao [20], and the dot-dashed line from Nelkin [21]. The scaling exponent,  $o_{p/3}$ , of  $\langle \Omega_r^{p/3} \rangle$  has also been plotted for comparison against  $p$  and shown by the (×) symbol. The inset shows the scaling relation  $\langle \varepsilon_r^p \rangle$  versus  $r$  for  $p$  from 1 to 10.

are  $\tau_{1/3} = 0.026$ ,  $\tau_{2/3} = 0.026$ ,  $\tau_{4/3} = -0.051$ ,  $\tau_2 = -0.223$ ,  $\tau_{8/3} = -0.483$ , and  $\tau_{10/3} = -0.822$ . Values of  $\tau_{p/3}$  for various available models [1,13,19–21] are also shown. For low-order moments ( $p \leq 7$ ), all phenomenological models agree with numerical results quite well. The models can be made to agree with the data better by adjusting the free parameter contained in them (for example, by changing the  $p$ -model parameter from  $0.7$  to  $0.719$ ).

To compare the scaling features of  $\langle \Omega_r^p \rangle$  with those of  $\langle \varepsilon_r^p \rangle$ , we plot in Fig. 4 the quantity  $\langle \Omega_r^p \rangle$ , for  $p = 2$  and  $p = 4$ , against  $\langle \varepsilon_r^p \rangle$ . The dashed lines represent  $\langle \Omega_r^p \rangle \sim \langle \varepsilon_r^p \rangle$ . The relative power laws can be identified in the scaling range [shown by the (●) symbol]. It appears clear that the exponents of the locally averaged enstrophy are larger than those of locally averaged dissipation. We have found that  $\langle \Omega_r^2 \rangle \sim \langle \varepsilon_r^2 \rangle^{1.56}$  and  $\langle \Omega_r^4 \rangle \sim \langle \varepsilon_r^4 \rangle^{1.47}$ . This result does not seem to support the prediction from the irreducible representation of the rotation group  $SO(3)$  for  $l = 0$  [14], according to which  $\langle \Omega_r^2 \rangle$  scales the same way as  $\langle \varepsilon_r^2 \rangle$ . If we define  $\langle \Omega_r^p \rangle \sim r^{o_p}$ , using the relative power relation between  $\langle \Omega_r^p \rangle$  and  $\langle \varepsilon_r^p \rangle$ , we can calculate  $o_p$  from  $\tau_p$ . The typical scaling exponents are  $o_{2/3} = 0.0415$ ,  $o_{4/3} = -0.08$ ,  $o_2 = -0.347$ , and  $o_{8/3} = -0.737$ . Here the error bar is less than 5%. In Fig. 3, we include  $o_{p/3}$  (the × symbol) as a function of  $p$ : the result is that  $o_{p/3}$  is smaller than  $\tau_{p/3}$  for  $p > 3$ .

As pointed out in [22], in addition to  $\varepsilon$  and  $\Omega$ , one can also construct other small-scale quantities from the low-order grouping of local velocity derivatives,  $\partial_\alpha u_\beta \partial_\gamma u_\delta$ . For incompressible fluids, it has been shown [14] that they can be decomposed on the basis of  $SO(3)$  and represented by irreducible representations characterized by an index  $l$  ( $l = 0, 1, 2, 3$ , and  $4$ ). In this notation,  $S^2$  and  $\Omega$  are two scalar quantities corresponding to

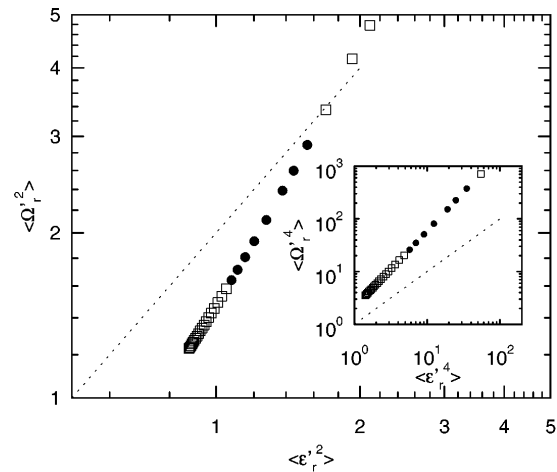


FIG. 4.  $\langle \Omega_r^2 \rangle$  as a function of  $\langle \varepsilon_r^2 \rangle$ . Here  $r$  is an implicit variable. The (●) points are for  $r$  in the inertial range ( $12 \leq r \leq 50$ ). The dotted line is for  $\langle \Omega_r^2 \rangle \sim \langle \varepsilon_r^2 \rangle$ . The inset shows a similar result for the fourth order quantity.

$l = 0$ . To understand the intermittency properties of these quantities with different  $l$  orders and compare them with those of  $\varepsilon_r$  and  $\Omega_r$ , we wish to construct local averages for  $l \geq 0$ . We show in Fig. 5 the scalings relative to  $\langle (S^2)_r^2 \rangle$  of various quantities with  $l$  orders up to 4. All these quantities have been averaged over the entire computational domain in all three directions, and thus well converged. According to [14], all these quantities should scale and the exponents should scale differently with the  $l$  order. We first note that these quantities do not all scale equally well at the Reynolds number of these simulations; this is no different when plotted directly against the averaging scale  $r$ . The quantity that scales best is  $\sum_i \langle (S_{ij} \omega_j)_r^2 \rangle$ , corresponding to  $l = 1$ . Among all the quantities considered, this quantity has a larger scaling exponent than all other quantities, which belong to a larger  $l$  order. In general, it would appear that the scaling exponents and intermittency appear to depend rather weakly on the decomposition index  $l$ , but that, at least for  $l = 1$ , the appearance of  $\omega$  in a scaling quantity renders it more intermittent.

Two concluding remarks are useful: First, the present results are based on direct numerical simulation at moderate Reynolds numbers. Caution should therefore be exercised when extrapolating them to high Reynolds numbers. In particular, the difference of the scaling exponent between the dissipation and enstrophy may not be adequately resolved until much higher Reynolds numbers have been reached. While the results available at high Reynolds numbers are consistent with the present results, the former [2] are based on one-dimensional surrogates. The effects of surrogacy are still far from being understood fully: for example, for the energy dissipation, the

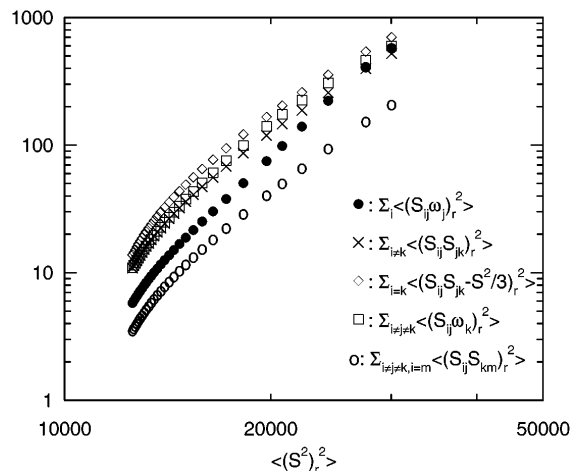


FIG. 5. Plotted against  $\langle (S^2)_r^2 \rangle$  are the quantities  $\sum_i \langle (S_{ij} \omega_j)_r^2 \rangle$  (filled circles,  $l = 1$ ),  $\sum_{i \neq k} \langle (S_{ij} S_{jk})_r^2 \rangle$  (crosses,  $l = 2$ ),  $\sum_{i=k} \langle (S_{ij} S_{jk} - S^2/3)_r^2 \rangle$  (diamonds,  $l = 2$ ),  $\sum_{i \neq j \neq k} \langle (S_{ij} \omega_k)_r^2 \rangle$  (squares,  $l = 3$ ), and  $\sum_{i \neq j \neq k, j=m} \langle (S_{ij} S_{km})_r^2 \rangle$  (open circles,  $l = 4$ ). Note that all the functions in this plot decrease as  $r$  increases.

surrogate field is in general more intermittent than the full field [3].

We thank N. Cao, H. Chen, V. L'vov, R. Kraichnan, I. Procaccia (especially), E. Titi, and J.-Z. Wu for useful discussions. Numerical simulations were carried out at the Advanced Computing Laboratory at Los Alamos National Laboratory and the Army High Performance Computing Research Center, using the Connection Machine-5. A grant from National Science Foundation supported the research work of K. R. S.

- [1] A. M. Obukhov, *J. Fluid Mech.* **13**, 77 (1962); A. N. Kolmogorov, *J. Fluid Mech.* **13**, 82 (1962).
- [2] K. R. Sreenivasan and R. A. Antonia, *Annu. Rev. Fluid Mech.* **29**, 435 (1997).
- [3] L.-P. Wang, S. Chen, J. Brasseur, and J. Wyngaard, *J. Fluid Mech.* **309**, 113 (1996); I. Hosokawa, S.-i. Oide, and K. Yamamoto, *Phys. Rev. Lett.* **77**, 4548 (1996).
- [4] S. Chen, G. D. Doolen, R. H. Kraichnan, and Z.-S. She, *Phys. Fluids A* **5**, 458 (1993).
- [5] A. N. Kolmogorov, *C. R. Acad. Sci. USSR* **32**, 19 (1941).
- [6] K. R. Sreenivasan, S. I. Vainshtein, R. Bhiladvala, I. San Gil, S. Chen, and N. Cao, *Phys. Rev. Lett.* **77**, 1488 (1996).
- [7] E. Siggia, *J. Fluid Mech.* **107**, 375 (1981).
- [8] R. Kerr, *J. Fluid Mech.* **153**, 31 (1985).
- [9] C. Meneveau, K. R. Sreenivasan, P. Kailasnath, and M. S. Fan, *Phys. Rev. A* **41**, 894 (1990); H. S. Shafi, Y. Zhu, and R. A. Antonia, *Phys. Fluids* **8**, 2245 (1996).
- [10] N. Cao, S. Chen, and K. R. Sreenivasan, *Phys. Rev. Lett.* **76**, 616 (1996).
- [11] J.-Z. Wu and M. Fan, *Constituents of Local Dissipation in Newtonian Fluid*, *Phys. Fluids* (1997 to be published).
- [12] H. Chen and S. Chen, *Phys. Fluids* (1997 to be published).
- [13] Z.-S. She and E. Leveque, *Phys. Rev. Lett.* **72**, 336 (1994).
- [14] V. L'vov and I. Procaccia, *Phys. Fluids* **8**, 2565 (1997); V. L'vov and I. Procaccia, preprint (1996).
- [15] N. Cao, S. Chen, and G. Doolen, *Phys. Fluids* (1997 to be published).
- [16] E. D. Siggia, *J. Fluid Mech.* **107**, 375 (1981); Z.-S. She, E. Jackson, and S. A. Orszag, *Nature (London)* **344**, 226 (1990); J. Jimenez, A. A. Wray, P. G. Saffman, and R. S. Rogallo, *J. Fluid Mech.* **255**, 65 (1993).
- [17] M. Brachet, *Fluid Dyn. Research* **8**, 1 (1991); G. R. Ruetsch and M. R. Maxey, *Phys. Fluids A* **4**, 2747 (1992); S. Kida and K. Ohkitani, *Phys. Fluids A* **4**, 1018 (1992); M. Tanaka and S. Kida, *Phys. Fluids A* **5**, 2079 (1993); T. Passot, H. Politano, P. L. Sulem, J. R. Angilella, and M. Meneguzzi, *J. Fluid Mech.* **282**, 313 (1995).
- [18] D. Y. Couder and M. Brachet, *Phys. Rev. Lett.* **67**, 982 (1991).
- [19] C. Meneveau and K. R. Sreenivasan, *Phys. Rev. Lett.* **59**, 1424 (1987).
- [20] S. Chen and N. Cao, *Phys. Rev. E* **52**, R5757 (1995).
- [21] M. Nelkin, *Phys. Rev. E* **52**, R4610 (1995); E. A. Novikov, *Phys. Rev. E* **50**, R3303 (1994).
- [22] E. D. Siggia, *Phys. Fluids* **24**, 1934 (1981).